Acta Cryst. (1976). B32, 47

The Modulated Structure of γ-Na_2CO_3 in a Harmonic Approximation

BY W. VAN AALST, J. DEN HOLLANDER, W. J. A. M. PETERSE AND P. M. DE WOLFF

Werkgroep Microstructuur, Lab. Technische Natuurkunde, Lorentzweg 1, *Delft, The Netherlands*

(*Received* 20 *January* 1975; *accepted* 7 *May* 1975)

Starting from the known average structure (Dubbeldam & de Wolff, *Acta Cryst.* (1969), B25, 2665–2667) and four-dimensional space group, the actual modulated structure has been determined by taking into account 758 newly measured main reflexions and 1152 first-order satellites. The analysis is based on a harmonic displacive modulation model, with 14 modulation parameters as well as 9 positional and 26 thermal parameters (individual anisotropic, in Debye–Waller factors of the usual type). The final value of $\sum\Delta/\sum F_o$ is 0·108 excluding, and 0·238 including non-observed reflexions. The main features of the modulation are (*a*) an overall modulation with an amplitude of close to 0·33 Å for all atoms except oxygen; (*b*) an orientational modulation of the CO_3 ion which is out of phase with the overall modulation. Calculation of the interatomic distances yields the result that the D_{3h} symmetry of the CO_3 ions is hardly distorted by the modulation. Certain second-order effects point to anharmonic components in the modulation, with amplitudes up to 0·03 Å. The structure turns out to consist of chains of NaO_6 octahedra sharing faces and with Na–O bond lengths under 2·45 Å, showing little variation. The chains run in the direction of **c** and are mutually coupled in other directions by CO_3 ions. The remaining Na atoms occupy the remaining spacious voids; their distances (averages $>2{\cdot}60$ Å) to eight out of the nine surrounding oxygen atoms vary strongly, and for each with a different phase.

1. Introduction

The diffraction pattern of γ-Na_2CO_3 has Laue symmetry $2/m$. Indeed a large number of reflexions – in particular those most prominent in the low-angle region – can be assigned to a normal monoclinic reciprocal lattice with basis vectors $\mathbf{a}^*, \mathbf{b}^*, \mathbf{c}^*$, $\mathbf{b}^*$ being perpendicular to $\mathbf{a}^*$ and $\mathbf{c}^*$. However, each of these 'main reflexions' is accompanied by a number of 'satellites' which can be described by introducing a fourth index m and an extra basis vector

$$\mathbf{q}^* = q_1\mathbf{a}^* + q_3\mathbf{c}^* \qquad (1)$$

in an extended form of the diffraction vector equation

$$\mathbf{H} = h\mathbf{a}^* + k\mathbf{b}^* + l\mathbf{c}^* + m\mathbf{q}^* \quad (h,k,l,m \text{ integer}) . \qquad (2)$$

Obviously q_1 and q_3 could be approximated by fractional numbers and suitable new axes could be chosen so as to retain triplets of integers instead of the above four. Such a procedure can be useful for descriptive purposes (*cf.* §10) but it has no physical meaning. Not only does it involve large index values and strange extinctions, but it cannot possibly cope with the fact that q_1 and q_3 in (1) are markedly and continuously dependent upon the temperature [Brouns, Visser & de Wolff (1964); *cf.* also Fig. 1 in the paper by de Wolff (1974)]. Therefore the addition of the fourth term in (2) must be regarded as essential.

The following systematic extinctions occur:

– Reflexions with $h+k$ odd are absent for all l and m.

– For $k=0$, all odd-order satellites (m odd) are absent (de Wolff & van Aalst, 1972). The presence of weak even-order satellites had formerly been overlooked; hence the erroneous statement in the earlier papers that no satellites at all appear for $k=0$.

Numerical values of parameters at room temperature are: $a=8{\cdot}904(3)$, $b=5{\cdot}239(2)$, $c=6{\cdot}042(2)$ Å; $\beta=101{\cdot}35(2)°$, $q_1=0{\cdot}182(1)$, $q_3=0{\cdot}318(1)$ where the vectors defined by a, b, c and β are reciprocal to the basis $\mathbf{a}^*, \mathbf{b}^*, \mathbf{c}^*$ and define what we call 'the unit cell'.

The anomalous satellite reflexions can be interpreted as the consequence of a displacive modulation, that is, a stationary lattice wave in which each of the atoms in the unit cell can have its own wave form, amplitude and phase but all have the same wave vector $\mathbf{q}^*$ defined by (1). This picture will be expressed in mathematical terms below [equations (3)···(8)]. The actual wave front is roughly parallel to $(20\bar{1})$ and the wavelength is about 16 Å. The fact that the intensity of satellites, though very irregular as a function of the indices, is on the whole very weak for $k=0$ and in general increases with increasing k indicates that displacements in the direction of **b** form an important component of the modulation.

In view of the prominence of main reflexions (at least for k up to 4) a first approximation to the structure can be obtained by disregarding the satellites. The electron density distribution so obtained is the average of the distributions in all unit cells. This 'average structure' was derived by Dubbeldam & de Wolff (1969). Since a and c are obviously not exact repeat translations of the actual structure, the average structure cannot be expected to consist of unambiguous atoms.

In fact, after a first trial with single atoms had failed, a satisfactory agreement was obtained when all atoms were equally divided over two positions; *cf.* Fig. 1. The space group of this average structure is $C2/m$, and the two positions of each atom are related to each other by the mirror plane. Only the layers $k=0\cdots3$

were taken into account, however, so that no conclusions could be drawn as regards the actual average distribution of atoms in the unit cell. In particular, a continuous distribution on a line connecting the two components of a split position could equally well explain the data available at the time.

In this respect, a peculiar situation exists with regard to the atoms O(1) and O(3). Fig. 2 shows the projection of the CO_3 ion along the line C–O(2). Both C and O(2) are very close to the mirror plane m and are drawn as single atoms (coinciding in this projection) for simplicity's sake. The split atoms O(1) and O(3), however, have distances of about 1 Å to the plane m. Assuming the CO_3 ion to be rigid, O(1) and O(3) will have to lie on a circle as shown. If a continuous distribution of these atoms exists, it seemed very likely that it would cover the short arcs ε rather than the very long arcs δ, since positions on δ would be incompatible with reasonable distances of O(1) and O(3) to the surrounding Na atoms (drawn schematically in Fig. 2 in order to show their relatively small distance to m planes).

Moreover, the fact that satellites for $k=0$ had not at that time been observed seemed to allow shifts in the **b** direction only, and thus to exclude intermediate positions both on the arcs ε and δ. The conclusion was drawn that O(1) and O(3) occupy discretely split positions, with little or no electron density in between. Hence the statement by Dubbeldam & de Wolff (1969) that the structure is of the domain type, with the two CO_3 orientations alternating in consecutive lamellar domains.

The observation of satellites for $k=0$ was a crucial point in the structure analysis, as it opened the possibility of a smooth distribution of O(1) and O(3) on the arcs ε. Accordingly, the domain structure hypothesis was given up. In terms of the modulation functions (*cf.* below) this meant that the square wave corresponding to the domain structure could now be replaced by much smoother types of periodic functions. The present paper describes the outcome of an analysis based on harmonic displacive modulation as a first approximation.

Regarding the definition and symmetry properties of modulated structures, our analysis will follow the general treatment published recently (de Wolff, 1974). In that paper, displacive modulation is defined by ordered displacements of the atoms of a normal reference structure. Let an atom of the ith kind be located, in the reference structure, at

$$\hat{\mathbf{r}}_i' = \hat{x}_i'\mathbf{a} + \hat{y}_i'\mathbf{b} + \hat{z}_i'\mathbf{c} \qquad (3)$$

with respect to an origin in a specified unit cell. Primed symbols are used for quantities depending on the unit cell in which the atom is situated. The displacement of this atom

$$\Delta_i' = u_i'\mathbf{a} + v_i'\mathbf{b} + w_i'\mathbf{c} \qquad (4)$$

is defined by

$$u_i' = u_i(\tau_i') \quad v_i' = v_i(\tau_i') \quad w_i' = w_i(\tau_i') \qquad (5)$$

u_i, v_i and w_i being the 'modulation functions'. These are periodic with a period of unity. Their argument τ_i' in (5) takes the value

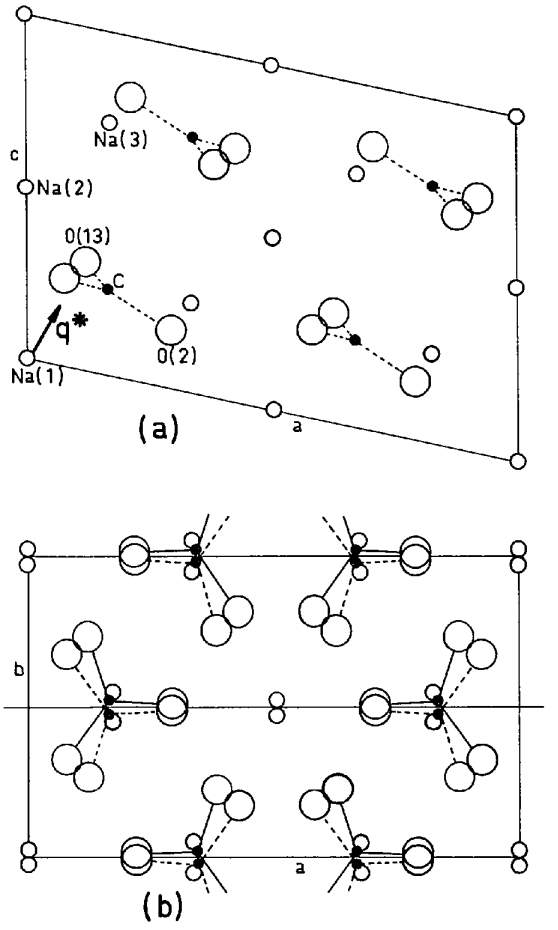

Fig. 1. The split-atom approximation of the average structure as determined by Dubbeldam & de Wolff (1969) (*a*) projected along **b**; (*b*) projected along **c**. Atoms are combined to CO_3 ions either by full lines or by broken lines; the other atoms shown are Na.

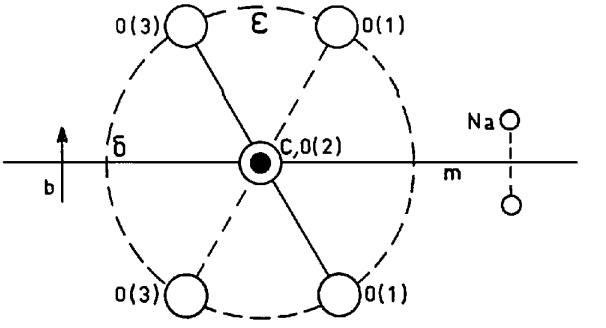

Fig. 2. Schematic projection along the direction C–O(2) of one CO_3 ion and a neighbouring Na atom. The overall shift of the anion and the rotation in its own plane [Fig. 1(*b*)] has been omitted here.

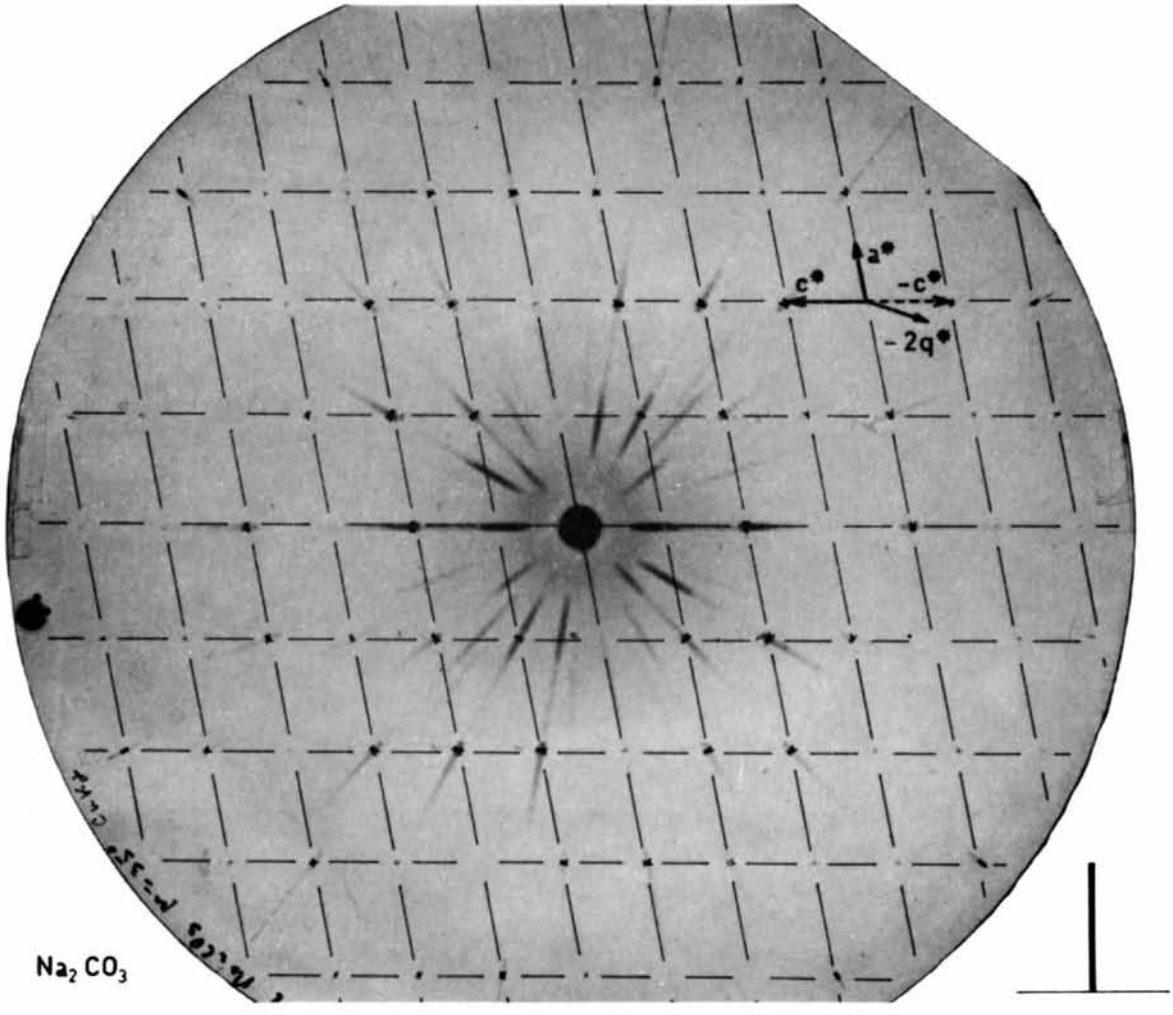

(*a*)

Fig. 3. Sections of the reciprocal lattice, taken from a series of photographs by Tuinstra & Fraase Storm (1972). (*a*), (*b*), (*c*): retigrams with lattice of main reflexions drawn in. The small plots represent the intensities of a main reflexion and its satellites, calculated from equation (20) with $V=0{\cdot}065$. (*a*) $k=0$, with some weak second-order satellites *e.g.* (4012) and (0032).

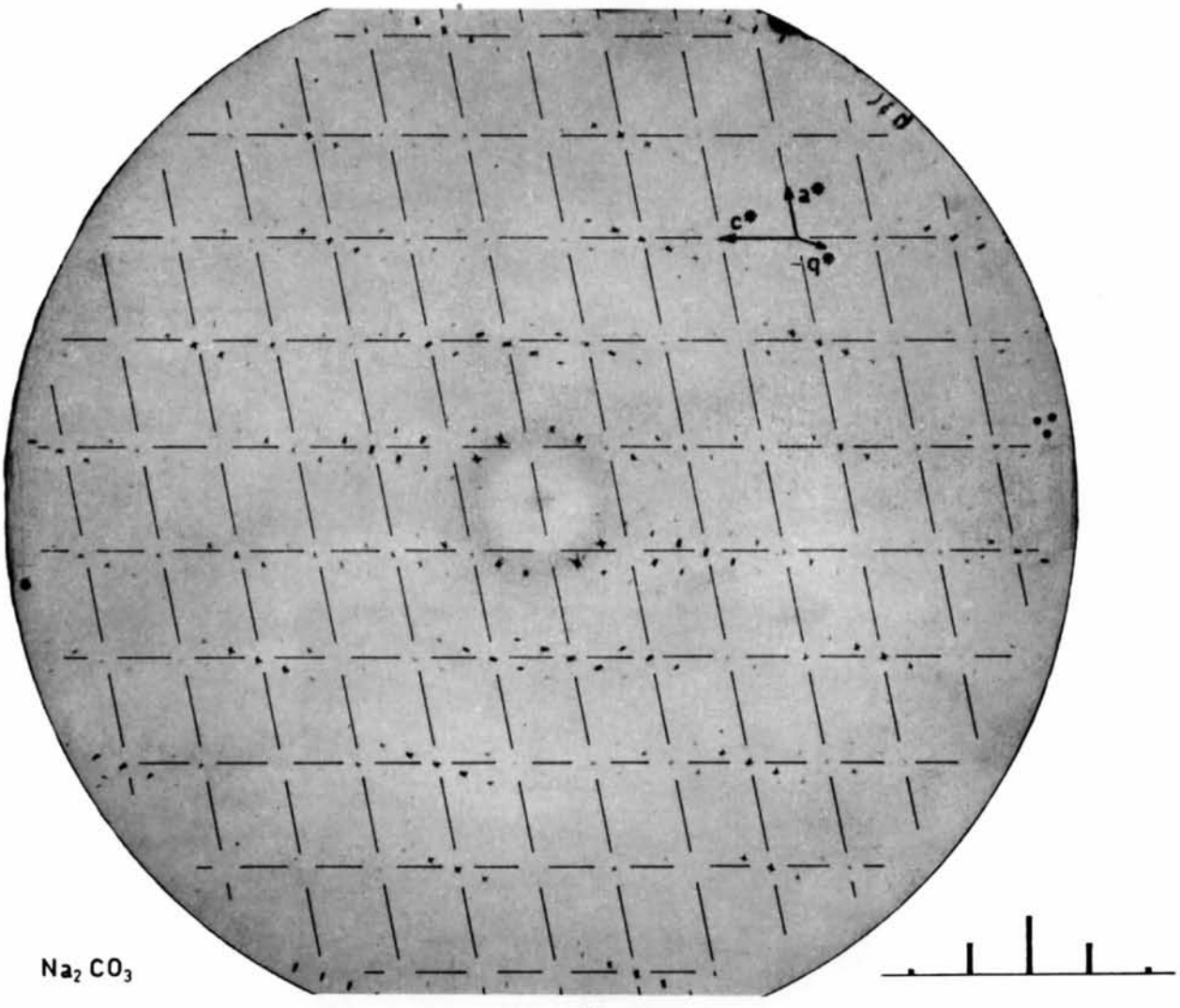

(*b*)

Fig. 3 (*cont.*) (*b*) $k=3$, a fourth-order satellite is visible near the centre $(132\bar{4})$.

$$\tau_i' = \mathbf{q}^* \cdot \mathbf{r}_i' \tag{6}$$

or

$$\tau_i' = q_1\hat{x}_i' + q_2\hat{y}_i' + q_3\hat{z}_i' \tag{7}$$

for the atom under consideration, while

$$\mathbf{q}^* = q_1\mathbf{a}^* + q_2\mathbf{b}^* + q_3\mathbf{c}^* \quad [cf. \text{ equation (1)}] \tag{8}$$

is a fixed vector. Satellites are thereby generated at points in reciprocal space given by equation (2). It is shown that the resulting modulated structure can be obtained as the intersection of normal space (R_3) with a four-dimensionally periodic structure in R_4, in which each atom is represented by a string running in the direction perpendicular to R_3. Periodic bending of each string (so as to make it follow a wavy line) accounts for the displacive modulation. This description is especially useful for symmetry considerations (*cf.* §3).

For the periodic functions we shall use the harmonic approximation:

$$u_i\tau = U_{ci} \sin 2\pi\tau + U_{si} \cos 2\pi\tau \,, \quad \text{and similarly for } v \text{ and } w. \tag{9}$$

It should be stressed that this is but an approximation. The actual modulation functions must contain higher harmonics (*cf.* §7), which will be the object of further research. The harmonic function (9) has, however, proved to be such a close approximation that separate publication of its results seems justified.

Of course one could replace (9) by expressions like

$$u_i = U_i \sin(2\pi\tau + \alpha_i) \quad v_i = V_i \sin(2\pi\tau + \beta_i) \quad w_i = W_i \sin(2\pi\tau + \gamma_i) \,. \tag{9a}$$

Since the field of parameters (U_i, α_i) has a singular branching line for $U_i = 0$, we prefer U_{si} and U_{ci} for the purpose of refinement.

2. Experimental

Small crystals of Na_2CO_3 were obtained by evaporation of an aqueous solution under a vapour pressure of about $1\frac{1}{2}$ bar. This was done in order to obtain a boiling point (about 120 °C) sufficiently far above the temperature (107 °C) where the anhydrous carbonate and the monohydrate are in equilibrium as solid phases under a saturated solution. The crystals were obtained as thin platelets, with a hexagonal shape (cross section up to 5 mm, thickness up to 0·3 mm), and parallel to the *ab* plane. Since Na_2CO_3 is extremely hygroscopic, crystals were sealed in Lindemann glass capillaries for exposure. From a suitable crystal fragment, retigrams were made of the layers $k = 0 \ldots 5$ (Cu $K\alpha$) and $6 \ldots 10$ (Mo $K\alpha$), (*cf.* Fig. 3) by Tuinstra & Fraase Storm (1972), using the Nonius retigraph. These photographs at once provided an important clue to the modulation (§6). Moreover they were extremely useful as reference material at all stages of the analysis.

Another fragment, roughly in the shape of a sphere $\varnothing = 0{\cdot}3$ mm was mounted on an Enraf–Nonius three-circle diffractometer. With this instrument, using Mo $K\alpha$ radiation, main reflexions and satellites for $h = 0 \ldots 16$, $k = 0 \ldots 10$, $l = -12 \ldots 12$ and $m = -4 \ldots 4$ were measured, about 10000 in all. For this purpose, the control program was modified so as to allow the addition of a fractional number mq_1 to h, and mq_3 to l.

All reflexions with the same value of m were measured in the same run. Absorption was neglected because of the approximate sphericity of the crystal with $\mu D \simeq 0{\cdot}17$.

3. Point group and space group

In terms of the indices h, k, l and m, the Laue symmetry $2/m$ is generated by the diagonal matrices

$$2' = \begin{pmatrix} -1 & & & \\ & 1 & & \\ & & -1 & \\ & & & -1 \end{pmatrix} \text{ and } m = \begin{pmatrix} 1 & & & \\ & -1 & & \\ & & 1 & \\ & & & 1 \end{pmatrix} \tag{10}$$

The prime in $2'$ stands for reversal of the sign of the fourth reciprocal coordinate m. In the point group of the actual four-dimensional structure, the matrices (10) operate on the coordinates in R_4. Because of Friedel's law, however, this point group need not be $2'/m$ but could also be either $2'$ or m (The prime now means sign reversal of the fourth coordinate in direct space.) In the latter case, one would expect the average structure to have the point group 2 or m, respectively, as it is just the projection of the structure in R_4 along the fourth basis vector. Since the average structure has been refined successfully in the point group $2/m$, the four-dimensional point group $2'/m$ can be assigned to the structure in R_4 with reasonable certainty. This assumption is further justified by the results of the present analysis.

Regarding the space group, the general extinction for $h+k$ odd (all l and m) shows the presence of a centring translation $(\frac{1}{2}\frac{1}{2}00)$ in the four-dimensional structure. The $2'$ operator is present as such, since there is no extinction in the row $(0k00)$. The mirror hyperplane, however, has to be a glide plane. As a matter of fact, a true mirror hyperplane in R_4 would create special positions which in the average structure would show up as splitting or smearing out *in* the corresponding plane in R_3. The actual splitting of positions in that plane, however, is in the direction perpendicular to the plane. Hence, the four-dimensional structure can have glide hyperplanes only.

Since the main reflexions $(h0l0)$ do not show any extinctions, the glide component of these mirrors must have the direction of the fourth base vector $\mathbf{a}_4$.* This conclusion was subtantiated by extra-long exposures

* After we published this derivation of the space group (de Wolff & van Aalst, 1972) it turned out that it had in essence been privately communicated to us in 1971 by Dr P. la Fleur (Nijmegen), to whom we had mentioned the problem. We are glad here to acknowledge Dr la Fleur's priority.

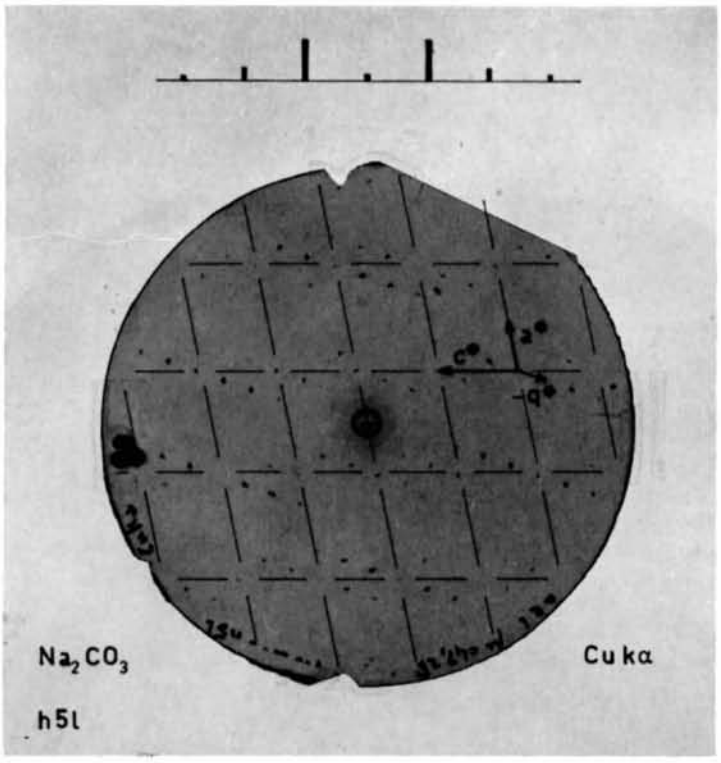

(*c*)

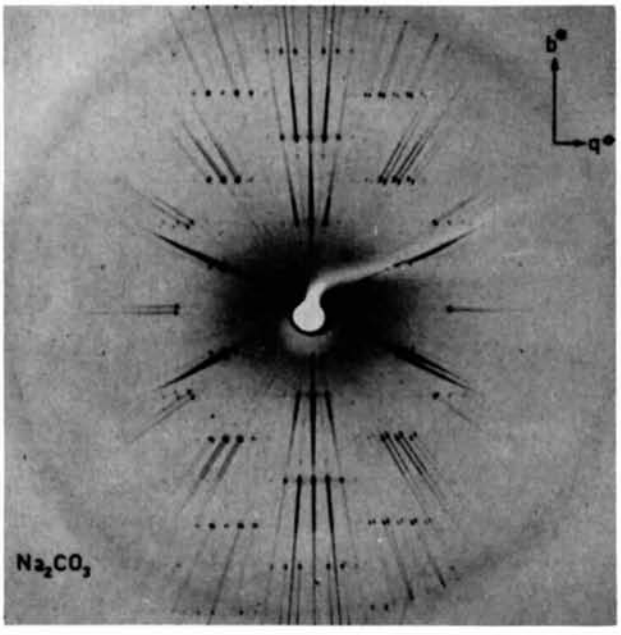

(*d*)

Fig. 3 (*cont.*) (*c*) $k=5$; (*d*) precession photograph, representing the plane containing all ($0k0m$) rows of reflexions. Other rows appearing in this picture are not in the plane and therefore have split reflexion spots.

[*To face p.* 49

which clearly demonstrate the extinction of $(h0lm)$ satellites with m odd, as mentioned in §1.

The resulting space group has the following eightfold general positions expressed in the coordinates x,y,z,ξ in R_4 [relative to basis vectors which are reciprocal to **a***, **b***, **c*** and **q***+**a**$_4$, *cf.* de Wolff (1974)], the origin being chosen in an inversion centre, whereas the lower part gives the coordinates used in §1, the primes on $\hat{x}$, $\hat{y}$, $\hat{z}$, u, v and w being left out for clarity's sake:

Four-dimensional

$(0000), (\frac{1}{2}\frac{1}{2}00)+$

x	y	z	ξ
$-x$	$-y$	$-z$	$-\xi$
x	$-y$	z	$\frac{1}{2}+\xi$
$-x$	y	$-z$	$\frac{1}{2}-\xi$

Three-dimensional

$(000), (\frac{1}{2}\frac{1}{2}0)+$ †

$\hat{x}+u(\tau)$	$\hat{y}+v(\tau)$	$\hat{z}+w(\tau)$
$-\hat{x}-u(-\tau)$	$-\hat{y}-v(-\tau)$	$-\hat{z}-w(-\tau)$
$\hat{x}+u(\tau+\frac{1}{2})$	$-\hat{y}-v(\tau+\frac{1}{2})$	$\hat{z}+w(\tau+\frac{1}{2})$
$-\hat{x}-u(-\tau+\frac{1}{2})$	$-\hat{y}-v(-\tau+\frac{1}{2})$	$-\hat{z}-w(-\tau+\frac{1}{2})$

(11)

It belongs to the triclinic system in R_4, and it is an extension of the arithmetic class No. 8 in the table by Fast & Janssen (1968).

4. Structure factor

One of us has shown (de Wolff, 1974) that the actual structure factor can be calculated by a four-dimensional Fourier transformation of the periodic structure in R_4. It should be kept in mind that in R_4, the atoms are not point- or sphere-like, but are represented by the strings mentioned in §1 and described by the equations (9). The scattering power of one atom, f_t, is smeared out along one period of the tth string. In the paper just mentioned, the structure factor for a single string is shown to be (with present notation, and leaving out the index t for convenience)

$$f\exp\{2\pi i(h\hat{x}+k\hat{y}+l\hat{z})\}\int_0^1 d\tau\exp[2\pi i\{(h+mq_1)u(\tau)+(k+mq_2)v(\tau)+(l+mq_3)w(\tau)+m\tau\}]\,. \quad (12)$$

We now introduce the harmonic modulation. Substitution of (9) changes the integral into

$$\int_0^1 d\tau\exp 2\pi i[(h'U_c+k'V_c+l'W_c)\sin 2\pi\tau+(h'U_s+k'V_s+l'W_s)\cos 2\pi\tau+m\tau] \quad (13)$$

where we have used the coordinates $h'k'l'$ of the diffraction vector

$$h'=h+mq_1 \quad k'=k+mq_2 \quad l'=l+mq_3\,. \quad (14)$$

If we define, moreover,

$$[(h'U_s+k'V_s+l'W_s)^2+(h'U_c+k'V_c+l'W_c)^2]^{1/2}=Z \quad (15)$$

$$\left.\begin{aligned}(h'U_c+k'V_c+l'W_c)/Z&=\cos 2\pi\zeta\\(h'U_s+k'V_s+l'W_s)/Z&=\sin 2\pi\zeta\end{aligned}\right\} \quad (16)$$

the integral (13) becomes

$$\int_0^1 d\tau\exp\langle 2\pi i\{Z\sin[2\pi(\tau+\zeta)]+m\tau\}\rangle=\exp\{2\pi im(-\zeta+\tfrac{1}{2})\}J_m(2\pi Z)\,. \quad (17)$$

Substitution in (12) and addition of the contribution of a centrosymmetrically situated string – as the second position in (11) to the first – gives *for this centrosymmetric pair*:

$$2(-1)^m f\cos\{2\pi(h\hat{x}+k\hat{y}+l\hat{z}-m\zeta)\}J_m(2\pi Z)\,. \quad (18)$$

While the above formula describes the general centrosymmetric case, those that follow (19...22) apply to the case in hand described by (11) and by $q_2=0$.

For the third atom of (11), the signs of $\hat{y}$ and of U_c, W_c, U_s and W_s have to be reversed. In (15) and (16), this yields parameters Z^- and ζ^- different from Z and ζ.

Hence the total structure factor *for the eightfold position* becomes:

$$4(-1)^m f[\cos\{2\pi(h\hat{x}+k\hat{y}+l\hat{z}-m\zeta)\}J_m(2\pi Z)+\cos\{2\pi(h\hat{x}-k\hat{y}+l\hat{z}-m\zeta^-)\}J_m(2\pi Z^-)]\,. \quad (19)$$

5. Positions in R_4

Since O(1) and O(3) are distributed over the arc ε in Fig. 2 (as explained in §1), the upper two half atoms in that figure together form a single string in R_4. Its image formed by the glide mirror hyperplane obviously consists of the lower two half atoms. Hence O(1) and O(3) together occupy a single general position. We shall denote this oxygen position as O(13) [short for O(1)+O(3)].

All other atoms have to occupy special positions, because their multiplicity is lower than 8. Looking in R_4 along the fourth basis vector **a**$_4$, the strings representing these atoms are projected (approximately) as the split atoms in the average structure. For all of them, the split atoms are very close to a mirror plane. Hence all these strings must coincide with their glide mirror images:

$$u(\tau)=u(\tau+\tfrac{1}{2}) \quad -v(\tau)=v(\tau+\tfrac{1}{2}) \quad w(\tau)=w(\tau+\tfrac{1}{2})$$

so $u(\tau)$ and $w(\tau)$ have even harmonics only. The function $v(\tau)$, on the other hand, has only odd-order Fourier coefficients. In the present case, and with harmonic modulation, this means that $U_c=U_s=W_c=W_s=0$; only V_s and V_c do not vanish for O(2), C, Na(3).

The strings for Na(1) and Na(2) are projected close

† To be read $\hat{x}\to\hat{x}+\frac{1}{2}$ and $\hat{y}\to y+\frac{1}{2}$ so that, according to (7), τ also changes!

to inversion centres. With their multiplicity 2, they must be invariant for the corresponding centres in R_4. *We choose a centre through which the* Na(1) *string passes as the origin in* R_4. Then $v(\tau)$ is an odd function, and for Na(1) and Na(2): $V_s=0$ as well; only V_c is left. The structure factors for these special positions are readily obtained from the general expression (19):

Fourfold position [O(2),C,Na(3)]: $\hat{y}=0$ or $\frac{1}{2}$ and $\beta=2\pi\zeta$ [equation (9*a*)], while $\zeta^-=\zeta$. The total contribution becomes:

$$(-1)^m 4f\cos\{2\pi(h\hat{x}+k\hat{y}+l\hat{z}-m\zeta)J_m(2\pi kV);$$
$$\tan(\zeta)=V_s/V_c;\quad V^2=V_c^2+V_s^2\,. \qquad (20)$$

Twofold position [Na(1), Na(2)]

$$\text{Na(1)}(\hat{x}=\hat{y}=\hat{z}=0)\colon (-1)^m 2fJ_m(2\pi kV_c) \qquad (21)$$

$$\text{Na(2)}(\hat{x}=\hat{y}=0,\ \hat{z}=\tfrac{1}{2})\colon (-1)^{m+l}2fJ_m(2\pi kV_c)\,. \qquad (22)$$

6. Determination of the modulated structure

The determination of the modulation parameters took a long time, because we only gradually became aware that the complete set, including all six parameters for the general O(13) positions, was indeed needed in order to describe the structure.

A first attempt was made at the time the domain type of modulation (*cf.* §1) was still believed to exist. Some 50 first-order satellites for $k=1$ and 2 each were measured, and all structure-factor contributions [including those for O(1) and O(3)] were supposed to have the form (20), with a parameter C_{ik} (depending on i and k only) in place of the Bessel function, and zero phase angles for Na(1) and Na(2) as in (21) and (22). The other phase angles ζ_{ik} were determined for each value of i and k separately, just as the C's. The search was performed by a Simplex program. A surprisingly good agreement was obtained, but some of the resulting C's and ζ's clashed with any model conceived so far. (The cause of this clash, it later appeared, was not so much the domain type hypothesis – since for low orders of reflexion, square-wave and sine functions are hardly distinguishable – but rather the assumption of rectilinear modulation models as discussed below.)

One of the major clues to the structure then came from the retigrams shown in Fig. 3. Looking at the dependence of the intensity on k and on m, the characteristic properties of Bessel functions of the kind occuring in (21) (as illustrated in the small plots in Fig. 3) were at once recognized in the retigrams for the higher k values. The departures from this trend increase with decreasing k. The parameter V_c involved in (21) can be estimated even by visual inspection and is found to be 0·065. This phenomenon could only be explained by assuming that the Na atoms (whose atom form factor decreases much less with increasing k than is the case for O and C) have almost pure harmonic modulation functions. In that case, the resemblance of the total structure factor to (21) can occur if V_c (or the phase angle ζ) of Na(3) vanishes like those of Na(1) and Na(2) do by symmetry, and if all three have about the same amplitude V_c.

A second attempt at parameter refinement was now made, using the harmonic approximation and with the above findings as starting data. The formula (19) had not yet been developed. Instead, a much simpler formula was used, based upon the supposition that for O(13):

$$U_s/U_c=V_s/V_c=W_s/W_c \text{ ('rectilinear modulation')} \qquad (23)$$

which means that O(13) is modulated along a straight line (in R_3). Without this supposition, the equations (9) define an ellipse in R_3 as the locus of O(13).* Fourier synthesis of the average structure had given indications that the locus is rather elongated, so that (23) seemed to be a reasonable approximation. However, for $k=1$ and 2 it proved impossible to obtain an agreement even approaching the quality of the first attempt.

Re-examination of that first result then showed that the C's and ζ's could be re-interpreted in terms of harmonic modulation so as to make some sense. In particular, it was reassuring to find that the results for all three sodium atoms (obtained from reflexions with $k=1$ and 2) agreed with the above-mentioned conclusions from the retigrams for $k>5$.

The remaining contradictions were intriguing, since all parameters should be re-interpretable, provided that condition (23) is fulfilled. On the other hand the peculiarities in the C and ζ parameters for oxygen and carbon could be explained qualitatively by assuming that the search program had adapted their values to a departure of O(13) from the rectilinear modulation (23). Unlike the parameters used later on, the C's and ζ's have this extra flexibility because their dependence on k is not fixed. Consequently, (23) was dropped, and the full expression (19) for 'elliptical modulation' was established and programmed. From then on, the search went smoothly.

7. Choice of reflexions for refinement

From the good agreement which at this stage was reached (using a Simplex program written originally by Dr J. W. Visser and elaborated by two of the present authors, v.A and den H.) it could safely be concluded that the modulation of all atoms is preponderantly harmonic, as in equation (9). However, second and higher harmonics of the functions u,v,w

* Indeed the three equations (9) in the two variables $\sin 2\pi\tau$ and $\cos 2\pi\tau$ are mutually consistent only if the determinant formed by the latter's coefficients plus the column u,v,w vanishes – which amounts to a linear equation in u, v and w. Hence the locus lies in a plane; that it is an ellipse then follows from any pair of the equations (9).

cannot all be zero. This is apparent both from a structural viewpoint and from experimental data:

(i) The rotation angle of the C–O(13) vectors, even over the short arc ε of Fig. 2 is so large (roughly 40° between extremes) that rigorous validity of the harmonic equations (9) would entail variations of C–O distances of at least 0·04 Å.

This is hardly acceptable for such a strong bond; hence we expect a second harmonic of that magnitude in the v component of O(13). The argument is essentially the same by which one obtains even harmonics in the vertical component of the movement of a pendulum, as will be set out in detail in the discussion of bond lengths in §10.

(ii) For second- and higher-order satellites there is sufficient correlation between F_o and F_c to substantiate the harmonic model. The agreement is, however, much less good than for $m=0$ and ± 1, see Fig. 4. The large and very significant discrepancies for $k=0, m=2$ demonstrate that some or all atoms have appreciable second harmonic terms in their u and w components as well, as explained below.

A more detailed analysis will now be given to show how the various harmonics affect the intensities of satellites.

Let us generalize (9) into

$$\begin{aligned} u(\tau) &= U_c \sin(2\pi\tau) + U_s \cos(2\pi\tau) + \mu(\tau) \\ v(\tau) &= V_c \sin(2\pi\tau) + V_s \cos(2\pi\tau) + \nu(\tau) \\ w(\tau) &= W_c \sin(2\pi\tau) + W_s \cos(2\pi\tau) + \lambda(\tau) \end{aligned} \qquad (24)$$

with the understanding that this is essentially a Fourier series expansion: the first two terms represent the first harmonic, and the last stands for the second and all higher harmonics. It is assumed that the averages of u, v and w over one period vanish, so that there is no constant term in the series.

Substituting (24) into the general structure factor formula (12) we find for the integral therein:

$$\int \mathrm{d}\tau \exp\langle 2\pi i\{Z \sin[2\pi(\tau+\zeta)] + m\tau + h'\mu + k'\nu + l'\lambda\}\rangle \qquad (25)$$

to be compared with (17) and with the same notation used there.

Suppose that, for all values of τ,

$$h'\mu + k'\nu + l'\lambda \ll 1, \qquad (26)$$

an assumption justified by the good agreement obtained by assuming harmonic modulation. Then we may approximate the corresponding factor of the integrand as follows

$$\exp\{2\pi i(h'\mu + k'\nu + l'\lambda)\} \simeq 1 + 2\pi i(h'\mu + k'\nu + l'\lambda). \qquad (27)$$

Moreover, we now write the Fourier expansion explicitly:

$$h'\mu + k'\nu + l'\lambda = \sum_{-\infty}^{+\infty} A_n \exp[2\pi i n(\tau+\zeta)] \qquad (28)$$

where $A_{-n} = A_n^*$, and on account of our assumptions $A_0 = A_1 = 0$. The origin is shifted by ζ for convenience.

Substituting (28) and (27) in (25), the integral is readily expressed in terms of Bessel functions. The complete result for the structure factor becomes, for one atom:

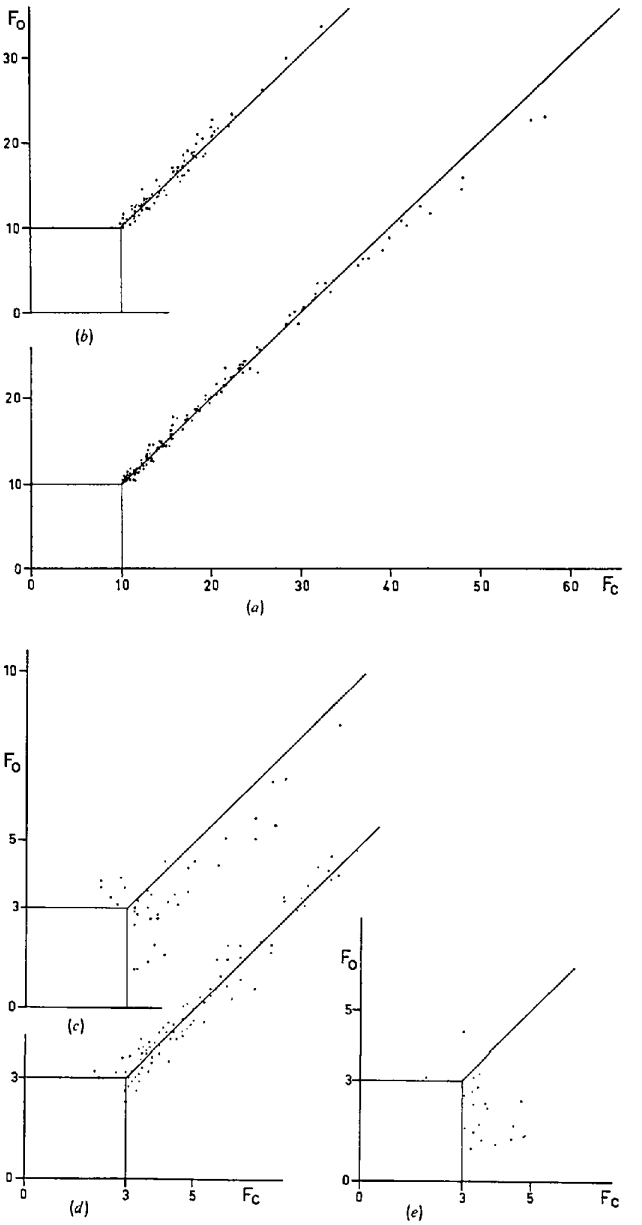

Fig. 4. Plots of F_o *vs* F_c for (*a*) $m=0$, (*b*) $m=\pm 1$ (all reflexions with $F>10$, except seven rejected because of strong extinction). Similar plots on a larger scale ($F>3$) demonstrate the difference in agreement for (*c*) second- and (*d*) first-order satellites, both representing the complete set with $k=2$ or 3. The second-order satellites for $k=0$ (*e*), though comparable in accuracy to (*d*), show a still weaker correlation.

$$F=f\exp\{2\pi i[h\hat{x}+k\hat{y}+l\hat{z}-m(\zeta+\tfrac{1}{2})]\}$$

$$\times[J_m(2\pi Z)+2\pi i\sum_{\substack{-\infty\\ n\neq 0,+1}}^{+\infty}A_nJ_{m-n}(2\pi Z)]\,. \quad (29)$$

The second term in the second factor is, of course, the (approximate) contribution of the anharmonic terms in (24).

In particular we find for the factor in square brackets in (29)

$$\text{for } m=0\text{: } J_0+4\pi i\{Re(A_2)J_2-iIm(A_3)J_3+\ldots\} \quad (30)$$

$$\text{for } m=1\text{: } J_1+2\pi i\{-A_2J_1+A_2^*J_3+A_3J_2+A_3^*J_4+\ldots\} \quad (31)$$

$$\text{for } m=2\text{: } J_2+2\pi i\{A_2J_0+A_2^*J_4-A_3J_1+A_3^*J_5+\ldots\} \quad (32)$$

where all Bessel functions have the same argument, *viz.* $2\pi Z$.

Since, by assumption (26), the coefficients A_n are small quantities, the bracketed sum in (30) and (31) is usually small compared with the first term. In (32), however, the term $2\pi iA_2J_0$ is much larger than the terms with A_2 in (30) and (31), at least for small Z where $J_0\gg J_1>J_2$. Striking discrepancies can be expected, even if A_2 is quite small. As stated above, such discrepancies do indeed occur. Expressions like (30–32) for third and higher-order satellites again contain terms with J_0, so these are as unreliable as the second-order satellites.

For this reason the refinement of the harmonic-model modulation parameters has been based on main reflexions and first-order satellites only.

8. The temperature factor

In our refinement, the effect of heat motion on the diffraction amplitudes has been accounted for by a Debye–Waller factor of the usual type, expressed as follows in the components $h'k'l'$ (14) of the diffraction vector:

$$\exp[-(b_{11}h'^2+b_{22}k'^2+b_{33}l'^2+2b_{12}h'k'+2b_{23}k'l+2b_{13}h'l')] \quad (33)$$

with individual tensors b_{ij} for Na(1), Na(2), Na(3), C, O(2) and O(13). The following symmetry restrictions on the tensor coefficients were introduced: for O(13): none; for the other atoms: $b_{12}=b_{23}=0$, just as if we were dealing with atoms [except O(13)] lying in the mirror plane of a normal structure.

This conventional procedure was used *ad hoc*, so its main justification is the good agreement thus obtained rather than any deep consideration of the heat motion in modulated crystals. Still, it can be elucidated to some extent on the basis of two experimental facts:

(i) Neither the main reflexion spots nor the satellites do show appreciable broadening. For large angles 2θ, reflexions of both kinds have been observed with separate Cu $K\alpha_1$ and α_2 spots hardly broader than the spectral width. Hence the modulation must have a long-range order no less perfect than the periodicity of good crystals of the normal type.

(ii) Localized diffuse scattering is observed in a wide range around the transition point at 360 °C (Tuinstra, 1974), but is extremely weak at room temperature. The general scattering, too, is quite normal as far as can be judged from our photographs.

It follows from (i) that the atomic positions in the modulated structure can be regarded as well-ordered equilibrium positions in which the thermal motion is centred. The absence of abnormal diffuse scattering [*cf.* (ii)] indicates, moreover, that the thermal motion does not show a behaviour greatly different from that of normal crystals. Diffuse thermal scattering may, here too, be peaked at the reflexion sites in reciprocal space – but this will not be apparent from the results of routine type of measurements such as we made.

Strictly speaking the actual thermal motion of an atom may well depend on the location of the unit cell in which it is situated, that is, on τ_i', *cf.* (7). In writing the factor as we have done in (33), we assume that this dependence has a negligible effect. If we had not done so, each b_{ij} of all six atoms would have had to be made a function of τ_i', and the above symmetry restrictions would have been replaced by relations between such functions. Fortunately, the present approximation has proved to be adequate for our purpose.

9. Results of least-squares refinement

For further refinement a least-squares program has been written by one of us (P.), using as the major subroutine the least-squares program *ORGLS* of Busing & Levy (1962). The latter had to be slightly modified to serve our purposes.

Attention has been paid to the structure factor calculation in order to save computer time: Bessel functions are not computed but are interpolated from tables; the structure-factor subroutine has two entries, one for each of the expressions (19) and (20); derivatives are computed numerically; the computation is economized in that each parameter is flagged when varied and only the contribution to the structure factor of flagged parameters is recomputed and added to the other contributions already stored in memory.

The final refinement has been obtained in different stages, starting from the values produced by the Simplex program mentioned in §7. Non-observed reflexions have not been taken into consideration. Firstly, individual isotropic temperature factors were refined in three cycles with 758 main reflexions. Thereafter all atoms were given anisotropic temperature factors, and the program was run for three more cycles.

Finally, the number of reflexions was extended to 1910 with the first-order satellites. Seven reflexions suspected of secondary extinction were omitted from this final list ($22\bar{2}0$, $3\bar{1}00$, $1\bar{1}20$, 0020, 2020, $40\bar{2}0$, $40\bar{1}0$). The positional and modulation parameters now were included in the refinement and in five cycles the program refined 50 variables to $S=1{\cdot}77$, where S is the accuracy indicator

$$S=\{\sum w\Delta^2/(n_o-n_v)\}^{1/2},$$

n_o = number of observations, n_v = number of variables, $\Delta=||F_{obs}|-|F_{calc}||$, $w=1/\sigma^2$, σ is standard error of F due to counting statistics. The final shifts were mostly smaller than the corresponding σ, and none was larger than 2σ.

The values of some other residuals after the last cycle are: $(\sum\Delta)/(\sum|F_{obs}|)=0{\cdot}108$ ($0{\cdot}080$ for $m=0$, and $0{\cdot}138$ for $|m|=1$), $(\sum w^{1/2}\Delta)/(\sum w^{1/2}|F_{obs}|)=0{\cdot}079$, $\{(\sum w\Delta^2)/(\sum w|F_{obs}|^2)\}^{1/2}=0{\cdot}070$. The final values of the parameters are listed in Table 1 (*a*) and (*b*). Table 2* lists F_o and F_c for all measured reflexions with $|m|=0$, 1 and 2. Separate plots of F_{obs} *vs* F_{calc} are presented in Fig. 4(*a*), (*b*) for $m=0$ and for $m=\pm1$. The former plot shows a trace of extinction for reflexions with $F_o>30$. The above set of seven rejected reflexions, all with $F_o>50$, had still greater discrepancies in the same sense. It is seen that the agreement for the satellites is hardly less good than it is for the main reflexions. This is brought out also by the value of S which is almost the same ($1{\cdot}15$ and $1{\cdot}19$ for $|m|=0$ and 1 respectively) as the above figure for the complete set. Fig. 4(*c*), (*d*), (*e*) illustrates the situation for second-order satellites, *cf.* §7.

* Table 2 has been deposited with the British Library Lending Division as Supplementary Publication No. SUP 31127 (26 pp., 1 microfiche). Copies may be obtained through The Executive Secretary, International Union of Crystallography, 13 White Friars, Chester CH1 Z1N, England.

10. Description of the modulated structure

In order to describe the modulated structure, one might draw a picture of the atomic positions in a large block of unit cells. We have actually done the calculation required, as will become apparent presently. However, a more condensed picture can be obtained by superimposing all these unit cells, while at the same time keeping track of the relation between the fractional atomic coordinates and the position of the unit cell in which the atom is situated. That relation follows directly from (7): moving from a given unit cell to another by a shift $n_1\mathbf{a}+n_2\mathbf{b}+n_3\mathbf{c}$ yields new displacements u',v',w' for each atom which are obtained by letting each τ_i' in (6) increase by the same number

$$n_1q_1+n_2q_2+n_3q_3\,. \qquad (34)$$

Because of the irrationality of at least one q_i (in our case, of q_1 and q_3) the fractional part of the number (34) can take virtually any value between 0 and 1. Hence the entire crystal can be represented by a single unit cell, provided that, for each atom in this cell, the coordinates are specified as periodic functions of a new variable, t:

$$u_i=u(\tau_i+t)\quad v_i=v(\tau_i+t)\quad w=w(\tau_i+t)\,. \qquad (35)$$

No primes are needed now since the τ_i refer to just one unit cell:

$$\tau_i=q_1\hat{x}_i+q_2\hat{y}_i+q_3\hat{z}_i$$

where the unprimed $\hat{x},\hat{y},\hat{z}$ coordinates may, as usual, be made fractional numbers.

In this mono-cell representation, the displacements u',v',w' of an atom in different unit cells are not shown explicitly, but they can be derived at once by putting t equal to the corresponding value (34).

The advantage gained is that all short-range relations between an atom and its environment can now be studied as a function of t, without one's having to go

Table 1. *Positional and thermal parameters and final modulation parameters*

(*a*) Final positional and thermal parameters ($\times10^4$), *cf.* also Table 4

	$\hat{x}$	$\hat{y}$	$\hat{z}$	b_{11}	b_{22}	b_{33}	b_{12}	b_{13}	b_{23}
Na(1)	0	0	0	39 (1)	122 (5)	79 (3)	0	20 (1)	0
Na(2)	0	0	5000	42 (1)	74 (5)	80 (3)	0	23 (1)	0
Na(3)	1706 (1)	5000	7478 (2)	50 (1)	148 (4)	157 (3)	0	30 (1)	0
C	1641 (2)	5000	2496 (3)	25 (1)	73 (6)	59 (4)	0	10 (2)	0
O(2)	2897 (2)	5000	1771 (3)	31 (1)	190 (6)	115 (3)	0	35 (2)	0
O(13)	1016 (2)	2940 (3)	2855 (2)	58 (2)	93 (7)	135 (3)	14 (4)	20 (2)	−8 (4)

(*b*) Final modulation parameters, expressed as $U_c, U_s \ldots W_s$ (9) and also as U, V, W, α, β, γ (9*a*)

		($\times10^4$)					
Na(1)	V_c	567 (4)			V	0·297 (2) Å	
Na(2)	V_c	656 (4)			V	0·344 (2)	
Na(3)	V_c	687 (3)	V_s	−57 (4)	V	0·361 (2)	β −4·8 (4)°
C	V_c	589 (6)	V_s	9 (7)	V	0·308 (3)	β 0·9 (7)
O(2)	V_c	244 (5)	V_s	−78 (5)	V	0·134 (3)	β −17·7 (11)
O(13)	U_c	−275 (2)	U_s	−184 (3)	U	0·295 (3)	α −146·2 (7)
	V_c	770 (4)	V_s	70 (5)	V	0·405 (2)	β 5·2 (4)
	W_c	−214 (3)	W_s	−374 (4)	W	0·260 (5)	γ −119·8 (5)

into the rather irrelevant question as to which unit cell of the crystal corresponds to a given value of t. In particular, interatomic distances as a function of t ('distance functions') will be used extensively in the following discussion.

The actual calculations have been made for 22 equidistant values of t at intervals of $\frac{1}{22}$. This unusual choice was made for purely opportunistic reasons; it stems from an approximate description of the modulated structure by a periodic superstructure with base vectors $\mathbf{A}=2\mathbf{a}+2\mathbf{c}$, $\mathbf{B}=\mathbf{b}$ and $\mathbf{C}=-7\mathbf{a}+4\mathbf{c}$. For the values of q_1 and q_3 at room temperature, the modulation vector $\mathbf{q}^*$ equals the reciprocal vector $\mathbf{A}^*$ to within the experimental accuracy. The supercell contains 22 unit cells. It has been used in order to allow the computation of distance functions using a normal program for calculating interatomic distances.

After these introductory remarks we shall now discuss the structure in three sections:

(i) *General aspects of the modulation*

Table 2 shows that the Na atoms and the carbon atom all have an amplitude V close to 0·33 Å. Their phases β, too, are almost equal. Considering the carbon atom as the centre of a rigid CO_3 ion, and disregarding for the moment the orientation of the latter, it can be concluded that the modulation very closely resembles a sinusoidal but otherwise homogeneous distortion of the entire structure, with an amplitude of 0·33 Å in the direction of **b**. We shall call this general aspect: the overall modulation.

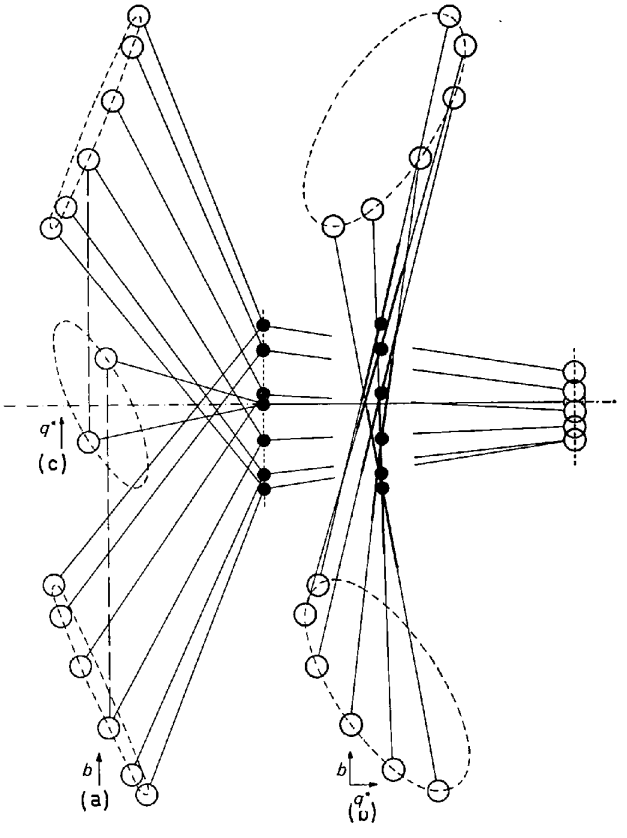

Fig. 5. Projections of the CO_3 ion. (*a*) along $\mathbf{q}^*$; (*b*) along the normal to **b** and $\mathbf{q}^*$; (*c*) along **b**. In (*b*), O(2) has been left out; it would fall on the same vertical line as carbon. In (*c*), O(2) is indicated on the mirror line. Six positions of the ion at intervals of $\frac{1}{11}$ in t are drawn in (*a*) and (*b*); only one of these six appears in (*c*).

The rigidity of the CO_3 ion is well confirmed by the relevant distance functions [*cf.* (ii) below]. Its orientational modulation however yields displacements differing entirely from the pattern of the general distortion just mentioned. This can be seen from Fig. 5, showing projections of the CO_3 ion in three mutually perpendicular directions two of which are along $\mathbf{q}^*$ and **b**. It so happens that the line connecting C and O(2) is perpendicular to $\mathbf{q}^*$ within the experimental accuracy, hence this system of axes is perfectly suited.

In each projection the locus of the O(13) atoms (one or two ellipses) has been drawn, as well as the rectilinear loci of C and O(2). The latter are both parallel to **b** and are therefore projected as a point in the **b** projection [Fig. 5(*c*)]. In Fig. 5(*b*) the two rectilinear loci coincide. Fig. 5(*a*) and (*b*) also show six positions of the actual CO_3 ion [Fig. 5(*c*) only one, for clarity's sake]. These six correspond to Nos. 1, 3, 5, 7, 9 and 11 of the above-mentioned set of 22 full coordinate lists at intervals of $\frac{1}{22}$ in t. The orientational modulation of each CO_3 is seen to consist of two components:

(1) A libration in its own plane with an amplitude of about 9°, roughly 13° out of phase with the overall modulation of the C atom, in a sense so as to reduce the amplitude of O(2).

(2) A libration about the direction C–O(2) with an amplitude of about 20°, roughly 45° out of phase with the overall modulation. [A third component of libration, about an axis parallel to **b**, is not excluded in principle but it cannot occur in the harmonic model which for O(2) and for C allows displacements parallel to **b** only, *cf.* §5.]

The second component is the one which corresponds to Fig. 2. Comparison of Fig. 5(*b*) with that stylized figure shows the considerable complexity caused by the additional overall translation and by the libration (1). The ensuing displacement of O(13) is by far the largest of all: its actual elliptical locus in space has a long axis of 1·01 Å and a short one of 0·40 Å.

(ii) *Configuration of the* CO_3 *ion*

For this section and the next one, the data on distance functions in Table 3 and Fig. 6 should be consulted. They are based on the results of the aforementioned supercell computation, in which all interatomic distances up to 3·3 Å have been calculated.

Apart from the average value of each distance, the fluctuations as revealed by the distance functions are of considerable interest. For our harmonic modulation model, we expect such fluctuations to be harmonic as well (that is, sinusoidal with a period of 1 in t). Second

Table 3. *Data on distance functions*

The letters *a*...*p* refer to Fig. 7.

		Min.	Max.	Average	Max.–Min.
C——O(2)	intra-CO_3	1·28	1·29	1·29	0·01*
C——O(13)	intra-CO_3	1·25	1·31	1·28	0·06
O(2)—O(13)	intra-CO_3	2·19	2·24	2·22	0·05
O(13)–O(13)	intra-CO_3	2·17	2·26	2·22	0·10*
Na(1)–O(2)	*a*	2·33	2·34	2·34	0·01*
Na(1)–O(13)	*b*	2·34	2·45	2·39	0·11
Na(2)–O(2)	*c*	2·42	2·44	2·43	0·02*
Na(2)–O(13)	*d*	2·31	2·36	2·33	0·05
Na(3)–O(2)	*e*	2·60	2·62	2·61	0·02*
Na(3)–O(2)	*f*	2·42	2·93	2·67	0·51
Na(3)–O(13)	*g*	2·34	2·92	2·63	0·59
Na(3)–O(13)	*h*	2·39	2·80	2·60	0·41
Na(3)–O(13)	*i*	2·65	3·25	2·95	0·59
Na(3)–Na(1)	*k*	3·03	3·05	3·04	0·02*
Na(3)–Na(2)	*l*	3·08	3·23	3·15	0·15
Na(1)–Na(2)	*m*	3·02	3·04	3·03	0·02*
O(2)—O(13)	*n*	3·06	3·26	3·16	0·20
O(13)–O(13)	*p*	3·09	3·15	3·12	0·07*

* These 'special distances' have the period ½ because of the glide mirror.

and higher harmonics can be caused only by the non-linear dependence of distance on the coordinates involved; they will usually have small amplitudes, and they have no direct structural significance.

In this respect, a distinction should be made between 'general' and 'special' distances. The name 'special' refers to a distance between a pair of atoms which – as a pair – is invariant for the glide mirror operator in R_4, such as the distance between both O(13) atoms of the same CO_3 ion. (An equivalent and more convenient criterion is: invariance of the pair in the average structure for the mirror plane of that structure.) It follows that a special distance, like the pair to which it belongs, is invariant for the glide mirror. Since the latter involves a shift of ½ in *t*, a special distance has the period ½ in *t*: with harmonic modulation, it can merely show the artificial fluctuations discussed above, and none of the more interesting first harmonic phenomena.

Regarding the CO_3 ion, a separate calculation shows the distance from C to the plane containing the three O atoms (which is a special distance in the above sense) to be as small as 0·002 Å. Hence the planarity of the anion is well confirmed. The C–O distances agree with recent data, *e.g.* on K_2CO_3 (Gatehouse & Lloyd, 1973).

The expected threefold symmetry axis, too, is corroborated, both by the C–O and by the O–O distance functions. Fig. 6 shows the prominent but artificial fluctuations (with period ½) of the special O(13)–O(13) distance. The fact that also the general distances C–O(13) and O(2)–O(13) show only second harmonic fluctuations supports the statement (i) in §7, namely that a considerable second harmonic term can be expected in the modulation functions of O(13) in order to compensate these improbably large fluctuations in the length of what are known to be strong bonds.

(iii) *Coordination of the* Na *atoms*

In Fig. 7, part of the structure projected along **b** has been redrawn in the same way as in Fig. 1(*a*). No great

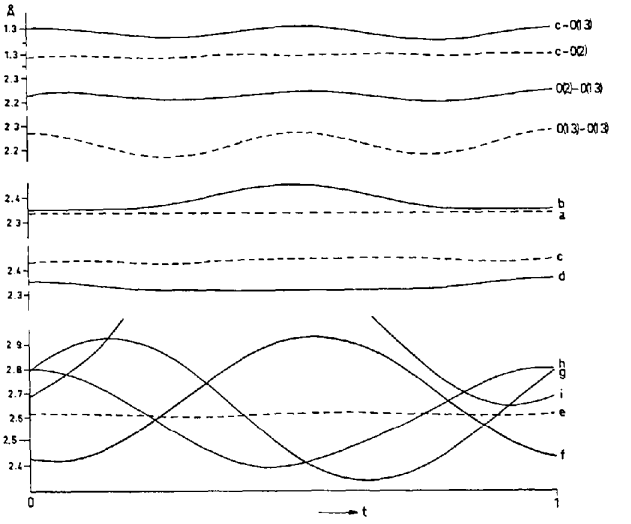

Fig. 6. Distance functions, *cf.* also Fig. 7 for the significance of the letters. Broken lines: special distances. Full lines: general distances.

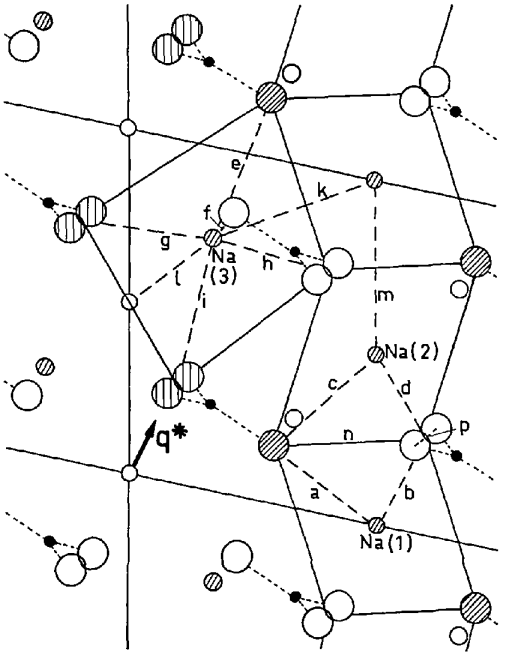

Fig. 7. Part of the structure redrawn as in Fig. 1(*a*). The two O(13) atoms of each CO_3 ion symbolize the actual modulated structure as shown in Fig. 5(*c*). The circumference of the octahedra surrounding Na(1) and Na(2) is drawn in full lines, so as to indicate the chain parallel to **c** which they form by sharing faces. Also the coordination of Na(3) by nine oxygen atoms (bond *e* single; *f*, *g*, *h* and *i* each representing two equivalent bonds) is indicated. Hatched: anions and Na at $y=\frac{1}{2}$; other: same at $y=0$.

significance should be attached to the two O(13) atoms appearing in this figure for each CO_3 ion; they symbolize the locus of O(13) which we now know to be the two ellipses of Fig. 5, coinciding in this projection [Fig. 5(*c*)]. They should be counted as one O atom about 1 Å above the average level of C and O(2), plus another about 1 Å below that level. Accordingly, we observe that both Na(1) and Na(2) have an unmistakable octahedral coordination by two O(2) and four O(13) each. The corresponding average distances are seen to lie between 2·33 and 2·43. Their fluctuations are small except for that of the general distance *b*. Even there, the general picture of octahedral coordination is well preserved.

For the Na(3) atoms, Fig. 7 at first sight seems to show an octahedron of surrounding O atoms as well, with one diagonal in the direction of the *b* axis. Looking closer, we observe that bonds *g*, *h* and *i* actually stand for two bonds each, directed to O atoms at a *y* level different from that of Na(3). Such a pair of equivalent bonds occurs indeed for every general distance. The two bonds of each pair are related by the glide mirror in R_4, so their distance functions are identical except for a phase difference of $\frac{1}{2}$ in *t*.

In all such cases, only one curve has been drawn in Fig. 6. The choice between the two possible phases was not relevant for bonds like C–O(13), *b* or *d*. In the case of Na(3)–O bonds, the choice has been made in such a way that the corresponding curves in Fig. 6 refer to bonds to the same Na(3) atom, with the same sign of their *y* component (that is, all pointing obliquely upward – or all downward – from the plane of Fig. 7).

Hence in total, nine O atoms are more or less involved in the coordination of Na(3). Except for the special distance *e*, however, all these bonds show huge fluctuations, so the actual coordination depends very strongly on the value of *t*. On the whole, it is much looser than that of Na(1) and Na(2).

Two general features can be detected in the structure:

(*a*) There is clearly a framework of chains, running in the direction of **c**, each consisting of alternating $Na(1)O_6$ and $Na(2)O_6$ octahedra sharing faces. The shortest O–O distances (not intra-CO_3) are actually the edges *n* and *p* of the shared faces (the next longer one has a minimum of as much as 3·21 Å). The chains are mutually connected, both in the direction of **b** and of **a**, by CO_3 ions. The Na(3) atoms occupy the remaining spacious voids.

(*b*) The strongest Na–O bonds are, on the whole, those which make the larger angle with the direction of **q***. This applies to bonds *a* and *d* of Na(1) and Na(2), as well as to those Na(3)–O bonds (*f*, *g* and *h*) which for some value of *t* become shorter than 2·50 Å.

An even stronger correlation with the direction of **q*** is shown by the tensor ellipsoids of the thermal motion.

In Table 4, the mean square amplitudes of thermal motion along the major ellipsoid axes are shown [approximately for O(13), neglecting b_{12} and b_{23}, and exactly for the other atoms]. Moreover, the angle φ between the *a* axis and the longer of the two major axes in the *xz* plane is listed. Comparing the latter with the corresponding azimuth of **q***, we observe that thermal motion in the *xz* plane is for all atoms anisotropic in the same way, with the strongest amplitude in a direction quite close to the vector **q***.

Table 4. *Mean square amplitudes* ($\times 10^4 A^2$) *of thermal motion in the directions of* **b** *and of the smaller and larger axes of the thermal ellipsoid*

The last column gives the angle φ between the larger axis and *a*. Errors in φ have been estimated from the errors in the other figures, which amount to 2–4%.

Major axis:	‖**b**	⊥**b** smaller	⊥**b** larger	φ (°)
Na(1)	169	115	165	44 (5)
Na(2)	103	113	179	42 (5)
Na(3)	206	175	285	74 (5)
C	101	91	109	68 (15)
O(2)	265	74	226	72 (3)
O(13)	128	222	242	69 (25)
				q*: 76·7

However, for the C and O atoms this correlation may be due to the fact that **q*** is perpendicular to the plane of the CO_3 ion. The relevant figures in Table 4 can be roughly accounted for by assuming a rigid-body thermal motion of the anion with small translational components, but with rather large librations about axes in its own plane as well as about its normal. The latter component produces mean square amplitudes of $\frac{1}{4}$ and $\frac{3}{4}$ for O(13), when those for O(2) are set at 1 and 0, in the first and second column of Table 4 respectively – which corresponds well with the trend observed in the actual figures. The thermal librations about the other axes merely contribute to the third column figures for the O atoms.

In this connexion it can be remarked that the correlation matrix produced by the refinement program shows considerable correlation (0·2–0·3) between b_{ii} and the modulation parameter for the *i*th axis (especially b_{22} and V_c) for all atoms – as expected, since for the main reflexions these parameters have a similar effect. Otherwise, correlation coefficients between thermal and either positional or modulation parameters are seldom larger than 0·05, which again seems to justify our treatment of thermal motion as a phenomenon distinct from the modulation and entirely comparable to that in normal crystals.

The authors wish to express their sincere gratitude for the cooperation and assistance of Dr H. van Koningsveld (measurements on the three-circle Nonius diffractometer of the Department of Chemical Technology, T. H. Delft, which we were kindly allowed to use), Dr J. W. Visser (Simplex program) and Ir P. Schippers (growing of crystals).

References

BROUNS, E., VISSER, J. W. & DE WOLFF, P. M. (1964). *Acta Cryst.* **17**, 614.

BUSING, W. R. & LEVY, H. A. (1962). *ORGLS. A General Fortran Least-squares Program.* Oak Ridge National Laboratory Report ORNL-TM-271.

DUBBELDAM, G. C. & DE WOLFF, P. M. (1969). *Acta Cryst.* B**25**, 2665–2667.

FAST, G. & JANSSEN, T. (1968). Technical Report 6-68, Katholieke Universiteit Nijmegen.

GATEHOUSE, B. M. & LLOYD, D. J. (1973). *J. Chem. Soc. Dalton*, pp. 70–72.

TUINSTRA, F. (1974). Private communication.

TUINSTRA, F. & FRAASE STORM, G. (1972). Internal report.

WOLFF, P. M. DE & VAN AALST, W. (1972). *Acta Cryst.* A**28**, S111.

WOLFF, P. M. DE (1974). *Acta Cryst.* A**30**, 777–785.

Acta Cryst. (1976). B**32**, 58

The Crystal and Molecular Structure of a Derivative of the Triterpene Spergulagenin A

BY T. AKIYAMA* AND J. V. SILVERTON

Laboratory of Chemistry, National Heart and Lung Institute, National Institutes of Health, Bethesda, Maryland 20014, *U.S.A.*

(*Received* 26 *March* 1975; *accepted* 9 *May* 1975)

12-*O*-Acetylspergulagenin A ethylene ketal, $C_{34}H_{56}O_6$, m.p. 265°C, orthorhombic, $P2_12_12_1$, $Z=4$, $a=9{\cdot}903$ (1), $b=15{\cdot}127$ (1), $c=21{\cdot}184$ (1) Å, $M=560{\cdot}8$, $D_m=1{\cdot}16$ (1) g cm^{-3}, $D_x=1{\cdot}174$ g cm^{-3}, 23°C, $\mu=6{\cdot}3$ cm^{-1}. Intensity data were collected with an automatic X-ray diffractometer. The structure was solved by direct methods including calculation of structure invariants and refined by least-squares methods to a final conventional R of 0·037. Spergulagenin A possesses a new migrated hopane skeleton with a methyl ketone moiety in the E ring as a side chain.

Introduction

Spergulagenin A (I), $C_{30}H_{50}O_4$, is a new triterpene which was isolated as one of the root sapogenols from *Mollugo spergula L.* Chemical and spectroscopic studies suggested that (I) had a migrated hopane or a lupane skeleton. In order to determine the chemical structure, an X-ray analysis of 12-*O*-acetylspergulagenin ethylene ketal (II) was undertaken. A preliminary report of this work has already been published (Kitagawa, Suzuki, Yosioka, Akiyama & Silverton, 1974).

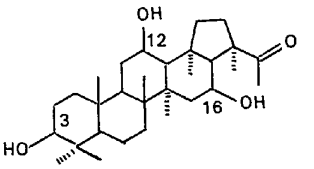

(I)

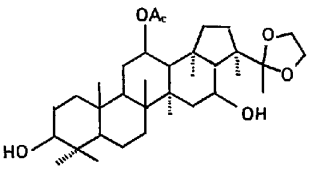

(II)

* Present address: Faculty of Pharmaceutical Sciences, University of Tokyo, Bunkyo-ku, Tokyo, Japan.

Experimental

Crystals were obtained by the conversion of spergulagenin A (I) to an ethylene ketal followed by partial acetylation. The product (II) was separated by chromatography and crystallized from ethanol as colorless prisms. Crystals used were ground to spheres (No. 1; $r=0{\cdot}2$ mm, No. 2; $r=0{\cdot}3$ mm). Cell dimensions were obtained by least-squares refinement using 15 Bragg angles measured at $\pm\theta$. (Cu $K\alpha$ X-radiation $\lambda=1{\cdot}5418$ Å) 3505 independent data (304 unobserved: 3σ) were measured (maximum sin θ/λ: 0·617 Å^{-1}) on an Enraf–Nonius CAD-4 diffractometer using techniques described by Silverton, Milne, Eaton, Nyi & Temme (1974). Three standard reflections, measured at intervals of every 45 reflections, showed some irradiation damage to be taking place and, after the intensities of the standards had dropped by 4%, the data crystal was replaced. The second crystal, used for about one third of the data, showed a drop of 2% in the intensities of the standards. The first data set was divided into two nearly equal parts and three scale factors, initially evaluated from the standards, were used as parameters in the refinement but final relative refined scale factors did not differ significantly from their original values. Lorentz and polarization corrections were applied but no corrections for absorption were made (no significant intensity changes were observed in azimuthal scans of several reflections.) The distribution of E values